

## *Ab Initio* Coupled-Cluster Effective Interactions for the Shell Model: Application to Neutron-Rich Oxygen and Carbon Isotopes

G. R. Jansen,<sup>1,2</sup> J. Engel,<sup>3</sup> G. Hagen,<sup>1,2</sup> P. Navratil,<sup>4</sup> and A. Signoracci<sup>1,2</sup>

<sup>1</sup>Physics Division, Oak Ridge National Laboratory, Oak Ridge, Tennessee 37831, USA

<sup>2</sup>Department of Physics and Astronomy, University of Tennessee, Knoxville, Tennessee 37996, USA

<sup>3</sup>Department of Physics and Astronomy, University of North Carolina, Chapel Hill, North Carolina 27516-3255, USA

<sup>4</sup>TRIUMF, 4004 Wesbrook Mall, Vancouver, British Columbia, V6T 2A3 Canada

(Received 10 February 2014; published 3 October 2014)

We derive and compute effective valence-space shell-model interactions from *ab initio* coupled-cluster theory and apply them to open-shell and neutron-rich oxygen and carbon isotopes. Our shell-model interactions are based on nucleon-nucleon and three-nucleon forces from chiral effective-field theory. We compute the energies of ground and low-lying states, and find good agreement with experiment. In particular, our computed  $2^+$  states are consistent with  $N = 14, 16$  shell closures in  $^{22,24}\text{O}$ , and a weaker  $N = 14$  shell closure in  $^{20}\text{C}$ . We find good agreement between our coupled-cluster effective-interaction results with those obtained from standard single-reference coupled-cluster calculations for up to eight valence neutrons.

DOI: 10.1103/PhysRevLett.113.142502

PACS numbers: 21.60.Cs, 21.10.-k, 21.30.Fe, 21.60.De

*Introduction.*—The nuclear shell model is the foundation on which our understanding of nuclei is built. One of the most important problems in nuclear structure today is to understand how shell structure changes with neutron-to-proton ratio throughout the nuclear chart. Shell structure influences the locations of the neutron and proton drip lines and the stability of matter. Examples of changes in shell structure are the appearance of new magic numbers  $N = 14$  and  $N = 16$  in the neutron-rich oxygen isotopes [1,2], and the emergence of an  $N = 34$  subshell closure in  $^{54}\text{Ca}$  [3–7].

Phenomenological shell-model Hamiltonians such as the *sd* Hamiltonian of Brown and Wildenthal [8,9] (abbreviated USD) and the *p-sd* Hamiltonian of Warburton and Brown [10] (abbreviated WBP), have successfully described properties of nuclei with proton number  $Z$  and neutron number  $N$  less than about 20. To understand the origin of shell structure, however, researchers are now trying to derive the shell model from realistic nucleon-nucleon (NN) and three-nucleon forces (3NFs), without further phenomenology [3,11,12]. Within the last few years, for example, Otsuka *et al.* [12] showed that 3NFs play a pivotal role in placing the drip line (correctly) in the oxygen isotopes at  $^{24}\text{O}$ , and Holt *et al.* [3] showed that inclusion of 3NFs can explain the high  $2^+$  state in  $^{48}\text{Ca}$ .

Until recently, all work to compute effective shell-model interactions was perturbative. Lately, however, nonperturbative calculations have become possible. In Holt *et al.* [13] core-polarization diagrams were summed to all orders, others have been based on the *ab initio* no-core shell model [14,15], via a valence-cluster expansion [16–18], and on the in-medium similarity renormalization group [19]. In this Letter we develop a new approach by using the *ab initio* coupled-cluster method [20–25], to construct effective

shell-model interactions for use in open-shell and neutron-rich nuclei. Starting from NN interactions and 3NFs generated by chiral effective-field-theory, we compute the ground- and excited-state energies of neutron-rich carbon and oxygen isotopes with up to eight neutrons in the valence space. Intense theoretical and experimental interest surround the structure of both these isotope chains, and particularly the neutron-rich carbon isotopes. Separation energies, spin assignments for low-lying states, the energies of  $2^+$  states, and transition rates in these isotopes all depend on the locations of shell gaps [26–33]. At present there is no evidence for a shell closure at the  $N = 14$  nucleus  $^{20}\text{C}$  [34], despite the  $N = 14$  shell closure at  $^{22}\text{O}$ . Furthermore, Efimov physics may be at play in  $^{22}\text{C}$  [35,36]. This Letter takes the first steps towards an *ab initio* shell-model description of the neutron-rich carbon isotopes, and addresses the role of 3NFs in these isotopes.

*Hamiltonian and model space.*—Our coupled-cluster calculations start from the intrinsic  $A$ -nucleon Hamiltonian,

$$\hat{H} = \sum_{i<j} \left( \frac{(\mathbf{p}_i - \mathbf{p}_j)^2}{2mA} + \hat{V}_{\text{NN}}^{(i,j)} \right) + \sum_{i<j<k} \hat{V}_{\text{3NF}}^{(i,j,k)}. \quad (1)$$

Here the intrinsic kinetic energy (the first term) depends on the mass number  $A \equiv Z + N$ . The potential  $\hat{V}_{\text{NN}}$  denotes the chiral NN interaction at next-to-next-to-next-to leading order [37,38] (with cutoff  $\Lambda = 500$  MeV), and  $\hat{V}_{\text{3NF}}$  is the 3NF that enters at next-to-next-to leading order with a local regulator [39] (with cutoff  $\Lambda_{\text{3NF}} = 400$  MeV). The low-energy constants of the 3NF are given by  $c_E = 0.098$  and  $c_D = -0.2$ . These were initially determined from a fit to the triton half-life and binding energy with a cutoff  $\Lambda_{\text{3NF}} = 500$  MeV [40], and then, with  $\Lambda_{\text{3NF}} = 400$  MeV,  $c_E$  was

readjusted to reproduce the  $^4\text{He}$  binding energy while  $c_D$  was kept fixed [41]. This introduces an inconsistency in the choice of regulator cutoff, but it has been shown [41–43] that with this cutoff, calculated binding energies agree rather well with data in the mass region we consider in this Letter. To achieve faster model-space convergence, we use the similarity renormalization group (SRG) to evolve  $\hat{V}_{\text{NN}}$  and  $\hat{V}_{\text{3NF}}$  to the lower momentum scale  $\lambda_{\text{SRG}} = 2.0 \text{ fm}^{-1}$  [44]. Many recent papers [41–43] have shown that this Hamiltonian reproduces binding energies of oxygen isotopes rather well; they vary by 1%–2% with variation of  $\lambda_{\text{SRG}}$ . However, this Hamiltonian has been shown to overbind for nuclei heavier than oxygen isotopes. Recent lattice nuclear effective field theory calculations [45] have shown that this overbinding might be due to a resolution scale that is too small, leading to interactions that are too soft in heavier nuclei. For the coupled-cluster calculations we used a Hartree-Fock basis built from  $N_{\text{max}} + 1 = 13$  major harmonic-oscillator orbitals ( $N_{\text{max}} = 2n + l$ ) with frequency  $\hbar\omega = 20 \text{ MeV}$ . We limit the number of 3NF matrix elements through the additional cut  $E_{3\text{max}} = N_1 + N_2 + N_3 \leq 14$ , where  $N_i = 2n_i + l_i$ . The resulting model-space is sufficient to obtain well converged results for energies of the states reported in this Letter. We use the normal-ordered two-body approximation for the 3NF [41,46], which has been shown to work well in light- and medium-mass nuclei [41].

*Formalism.*—To derive an effective shell-model Hamiltonian in a valence space from *ab initio* coupled-cluster theory, we use the valence-cluster expansion first applied in the no-core shell model [17,47]. We expand the Hamiltonian in Eq. (1) in a form suitable for the shell model:

$$H_{\text{CCEI}}^A = H_0^{A,A_c} + H_1^{A,A_c+1} + H_2^{A,A_c+2} + \dots, \quad (2)$$

where CCEI stands for coupled-cluster effective interaction,  $A$  is the mass of the nucleus we wish to treat, and  $A_c$  is the mass of the nucleus with a closed core below the valence space. In Eq. (2),  $H_0^{A,A_c}$  is the Hamiltonian for the core,  $H_1^{A,A_c+1}$  is the valence one-body Hamiltonian, and  $H_2^{A,A_c+2}$  is the additional two-body piece. In this work we limit ourselves to one- and two-body terms in the valence-space shell-model Hamiltonian. To solve for the ground state of the core nucleus  $A_c$  we use the coupled-cluster method in the singles-and-doubles approximation (CCSD) with the  $\Lambda$ -triples correction treated perturbatively [ $\Lambda$ -CCSD(T)] [48,49]. To obtain the ground and excited states for the  $A_c + 1$  and  $A_c + 2$  nuclei we use particle-attached and two-particle attached equation-of-motion (EOM) coupled-cluster methods [50–52]. For the particle-attached EOM we truncate at one-particle and two-particle-one-hole excitations, and for the two-particle attached EOM we truncate at two-particle and three-particle-one-hole excitations. In coupled-cluster theory the basic ingredient is the similarity-transformed Hamiltonian  $\bar{H} = e^{-T} H e^T$ , which is inherently non-Hermitian [53], thus we need to solve for the left and right eigenstates to obtain a complete *bi*-orthogonal set of states.

From the left and right eigenstates we can write Eq. (2) in a spectral representation.

The valence-space representation of Eq. (2) consists of a core energy term [which we compute from  $H_0^{A,A_c}$  using  $\Lambda$ -CCSD(T)], a one-body term (built from the particle-attached eigenvalues of  $H_1^{A,A_c+1}$ ), and a two-body term. The two-body term is computed using the Okubo-Lee-Suzuki similarity transformation [54–57] by projecting the two-particle attached EOM eigenstates onto two-body valence-space states. The Okubo-Lee-Suzuki projection of  $H_2^{A,A_c+2}$  onto the model space is [47,57]

$$\langle \alpha_P | \overline{H_{\text{eff}}^A} | \alpha_{P'} \rangle = \sum_{k=1}^d \langle \alpha_P | R_k^{A,A_c+2} \rangle e_k \overline{\langle \alpha_{P'} | R_k^{A,A_c+2} \rangle}. \quad (3)$$

Here the  $|R_k^{A,A_c+2}\rangle$  are the two-particle attached EOM eigenstates with eigenvalue  $e_k$  for  $A_c + 2$  (with mass  $A$  of the target nucleus in the kinetic energy),  $|\alpha_P\rangle$  are the model-space states, the sum is over the  $k$  two-particle attached eigenstates that have the largest overlap with the model space. The  $\langle \alpha_P | R_k^{A,A_c+2} \rangle$  are the matrix elements of the operator  $\mathbf{X}$ .  $\overline{\langle \alpha_{P'} | R_k^{A,A_c+2} \rangle}$  denote the matrix elements of the inverse of  $\mathbf{X}$ . To obtain the effective two-body shell-model interaction, we subtract the one-body part from Eq. (3) to avoid double counting.

Note that we could also construct an effective Hamiltonian using the corresponding left eigenvectors. This introduces an ambiguity in the construction of  $\overline{H_{\text{eff}}^A}$ . We have verified, however, that in this work the matrix elements of the effective operator are almost identical for either choice. The effective Hamiltonian in Eq. (3) is not Hermitian. Current shell-model codes require Hermitian matrices. To obtain a Hermitian representation of the effective shell-model Hamiltonian we construct the metric operator  $S^\dagger S$  where  $S$  is a matrix that diagonalizes  $H_{\text{CCEI}}^A$ ; the Hermitian shell-model Hamiltonian is then  $[S^\dagger S]^{1/2} H_{\text{CCEI}}^A [S^\dagger S]^{-1/2}$  [47,58].

*Results.*—Here we report our CCEI results for ground and low-lying states in oxygen and carbon isotopes. We choose  $^{16}\text{O}$  in oxygen and  $^{14}\text{C}$  in carbon as the closed-shell cores. We then project the one- and two-particle attached coupled-cluster wave functions onto the one- and two-particle model space states in the valence space—the  $d_{5/2}$ ,  $s_{1/2}$ ,  $d_{3/2}$  shell—and proceed to use the resulting shell-model Hamiltonians in heavier isotopes.

We would like to gauge the accuracy of our CCEI approach by comparing with full  $\Lambda$ -CCSD(T) calculations, the results of which we refer to as reference values.  $\Lambda$ -CCSD(T) is known to be accurate to within 1% [45]. Figure 1 shows the ground-state energies of all oxygen isotopes  $^{16-25}\text{O}$  computed with the CCEI (red squares), experimental ground-state energies (black circles), and the  $\Lambda$ -CCSD(T) ground-state energies in  $^{16-18,21-25}\text{O}$ . Our  $\Lambda$ -CCSD(T) calculations use the model space mentioned earlier, while the calculations that determine our CCEI use

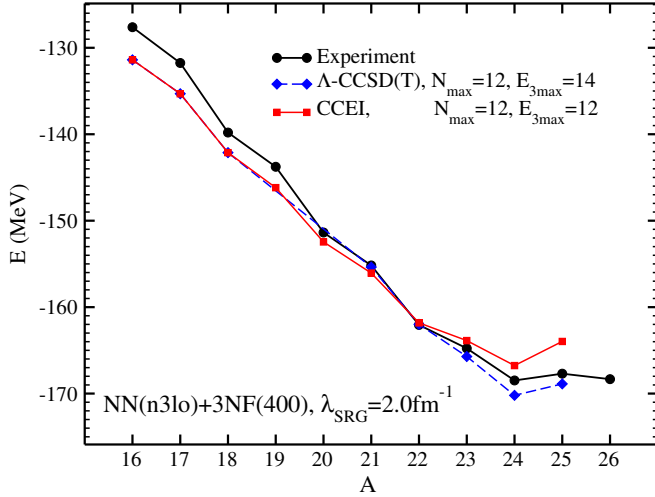


FIG. 1 (color online). Ground-state energies of oxygen isotopes. Black circles show the experimental values, blue diamonds the  $\Lambda$ -CCSD(T) results, and the red squares the CCEI results for the ground-state energies.

$N_{\max} = 12$  and  $N_1 + N_2 + N_3 = 12$ . We believe that our CCEI results are converged to within  $\sim 100$  keV, but increasing with the number of nucleons. Both our  $\Lambda$ -CCSD(T) and CCEI results are in rather good agreement with experimental binding energies. Our CCEI and  $\Lambda$ -CCSD(T) calculations also agree well with a variety of recent calculations in the oxygen isotopes that start with the same Hamiltonian [42,43].

If we look more closely, we see that the reference  $\Lambda$ -CCSD(T) results in  $^{21,22}\text{O}$  are in excellent agreement with our CCEI results. In  $^{23-25}\text{O}$  the CCEI results start to deviate from the  $\Lambda$ -CCSD(T) reference values. In  $^{24}\text{O}$  the CCEI ground state is about 3.5 MeV less bound than the  $\Lambda$ -CCSD(T) result, which amounts to roughly 2% of the total binding energy. In  $^{25}\text{O}$  the difference increases to about 3%. The difference indicates that effective three-body interactions induced by the Okubo-Lee-Suzuki transformation (which we neglect) start to play a role in the CCEI approach when the number of valence nucleons gets too large. The problem can be remedied by including these interactions or by increasing the valence-space size [17].

Next, we compare low-lying CCEI excited-state energies in  $^{22}\text{O}$  and  $^{24}\text{O}$  with an EOM coupled-cluster calculation that includes single and double excitations [59]. EOM-CCSD can accurately describe low-lying states that are dominated by one-particle-one-hole excitations [53], and we therefore choose those states for comparison. In  $^{22}\text{O}$  we obtain low-lying  $2^+$  and  $3^+$  states with 2.5 MeV and 3.5 MeV of excitation energy. The CCEI result for the same states is 2.7 MeV and 4.0 MeV, though the CCEI result for the  $3^+$  state in  $^{22}\text{O}$  is not yet converged; it moves down by  $\sim 150$  keV when we increase the model space size from  $N_{\max} = 10$  to  $N_{\max} = 12$  oscillator shells. The  $2^+$  state changes only by  $\sim 5$  keV indicating that it, by contrast, is well converged. In  $^{24}\text{O}$ , the  $2^+$  state is found by

EOM-CCSD at 6.0 MeV, while CCEI finds the same state at 5.7 MeV, a difference of about 5%. We observe that the differences in excitation energies between EOM-CCSD and CCEI remain small even though the difference in total binding energy increases significantly around  $^{24}\text{O}$ . All in all we estimate the total uncertainty in the excitation energies to be no more than 10%, based on the numbers presented above. Finally, we note that in our CCEI calculations, correlations between all particles in the valence space are treated exactly. Therefore, we expect to see some differences in the computed spectra using EOM-CCSD and CCEI. For example, in CCEI we are able to compute the second  $0^+$  state in  $^{22}\text{O}$  which is dominated by two-particle-two-hole excitations from the ground state. On the other hand this state is poorly described by EOM-CCSD.

We turn now to carbon. The  $\Lambda$ -CCSD(T) ground-state energies of  $^{14,15,16}\text{C}$  are  $-104.0$  MeV,  $-104.2$  MeV, and  $-106.6$  MeV, respectively. In  $^{14}\text{C}$  the result agrees well with the experimental ground-state energy of  $-105.3$  MeV, but for  $^{15,16}\text{C}$  our particle-attached and two-particle attached EOM results are 2.3 MeV and 4.2 MeV underbound with respect to experimental data. The underbinding persists throughout the chain of carbon isotopes in our CCEI calculations.

Figures 2 and 3 summarize our CCEI results for the excited states in  $^{19-24}\text{O}$  and  $^{17-22}\text{C}$ , respectively. For the first  $2^+$  states we also show the 10% conservative error estimate. Our results are overall in rather good agreement with experiment. Without any adjustment of parameters we obtain spectra that are qualitatively similar to those produced by the phenomenological USD (WBP) Hamiltonian for oxygen (carbon) isotopes. Our  $2^+$  energy at 2.78 MeV in  $^{22}\text{O}$  and at 5.73 MeV in  $^{24}\text{O}$  are consistent with a  $N = 14$  subshell and a  $N = 16$  shell closure in oxygen. On the other hand, the  $2^+$  energy at 1.72 MeV in  $^{20}\text{C}$  is consistent with a weaker  $N = 14$  subshell closure in carbon.

In the odd isotopes  $^{17,19,21}\text{C}$  we get the  $1/2^+$  state in the wrong position. Our calculations, however, rely on an underlying harmonic-oscillator basis and therefore do not account for the particle continuum. The  $1/2^+$  state is dominated by  $s$ -waves and is located close to the particle emission threshold, where continuum effects are obviously important [5,60]. The  $3/2^+$  and the  $5/2^+$  states are dominated by  $d$ -waves, which couple somewhat less to the continuum because of the  $l = 2$  centrifugal barrier [60]. Overall, we expect continuum effects to be quite significant for the  $^{17,19,21}\text{C}$  isotopes. Preliminary calculations within the no-core shell model with continuum [61] for  $^{17}\text{C}$ , with the same chiral  $NN + 3NF$  interaction used here, show that the  $1/2^+$  state (unbound in our calculation) gains about 2 MeV in energy and becomes bound. At the same time, the  $3/2^+$  and  $5/2^+$  states are lowered in energy by more than 1 MeV. We anticipate similar or even stronger continuum effects in  $^{19}\text{C}$  and  $^{21}\text{C}$ ; these would most likely make the  $1/2^+$  states the ground states, as they are in reality.

*Summary.*—We have used coupled cluster theory to derive shell-model Hamiltonians that depend on no

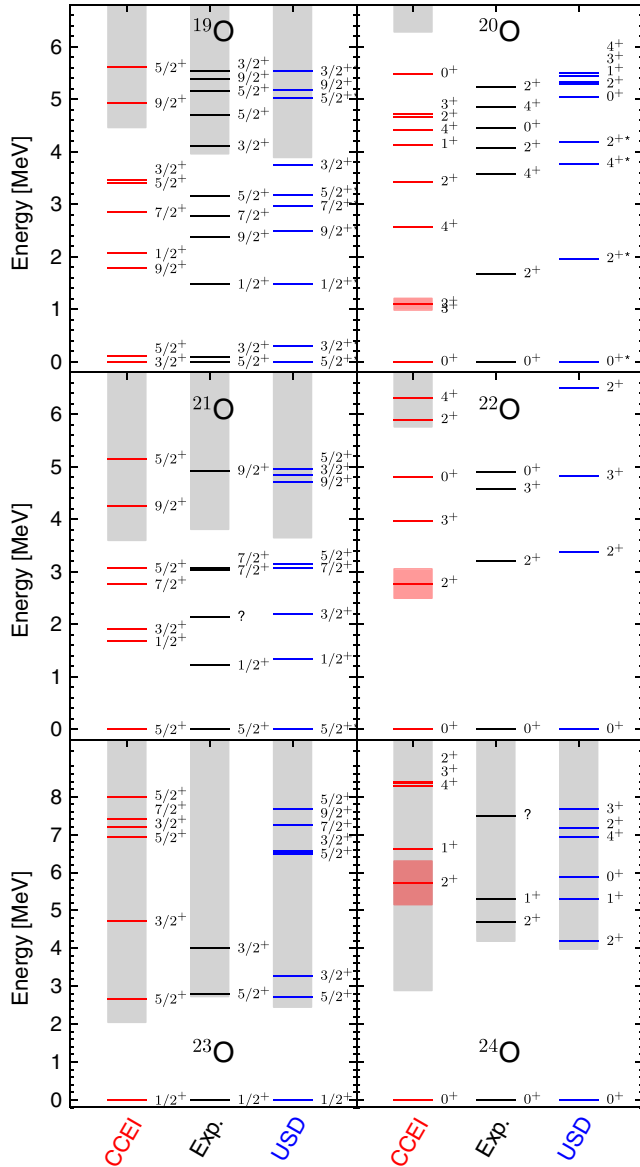


FIG. 2 (color online). Excitation spectra of neutron-rich oxygen isotopes. The left columns (red lines) contain the CCEI results, the middle columns (black lines) the known experimental data, and the right columns (blue lines) the spectra obtained with the USD shell-model Hamiltonian [8,9]. A star next to the excitation levels in the right columns indicates that the level was included in the fit of the USD Hamiltonian. The gray bands indicate the neutron decay thresholds, and the shaded area centered around the first  $2^+$  states show the 10% error estimate discussed in the text.

parameters other than those in the initial chiral NN interaction and 3NF. We have reproduced ground- and excited-state energies with good accuracy in carbon and oxygen isotopes. The results demonstrate both the predictive power of Hamiltonians from chiral effective field theory and the accuracy of the coupled cluster framework. Finally, our shell-model calculations can and will be systematically improved (e.g., by including induced three-body interactions), extended to include effective

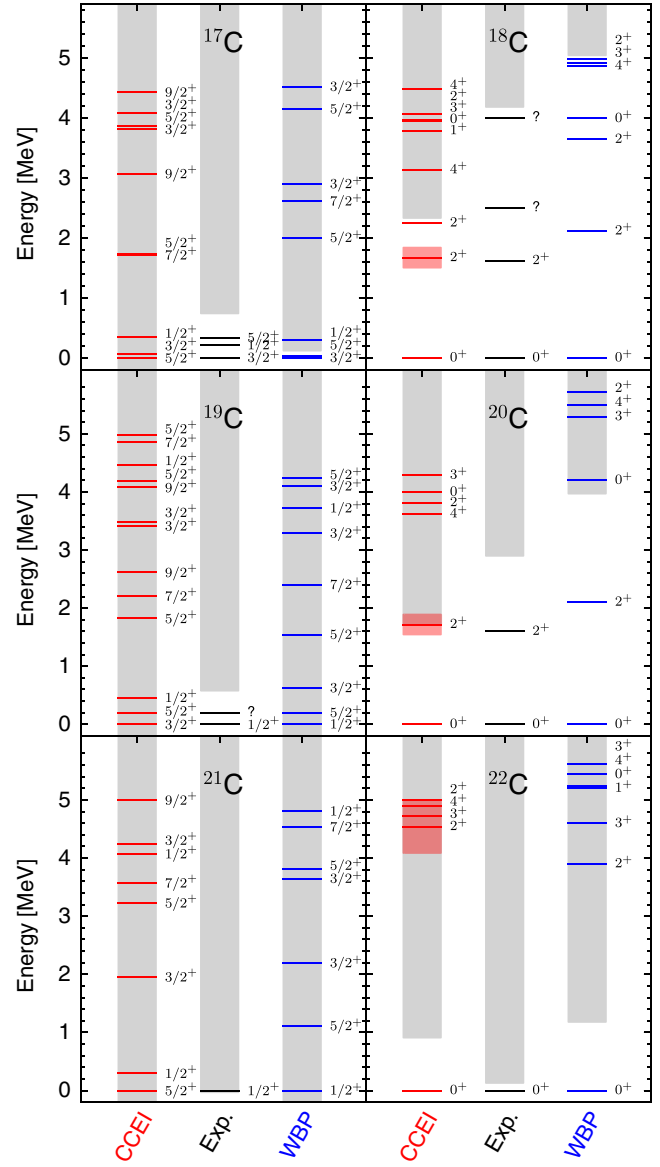


FIG. 3 (color online). Same caption as in Fig. 2 except for carbon isotopes. The right columns (blue lines) show the spectra obtained with the WBP shell-model Hamiltonian [10].

operators other than the Hamiltonian, and applied to heavier nuclei, where accurate phenomenological Hamiltonians are harder to obtain.

We thank Scott Bogner, Morten Hjorth-Jensen, Thomas Papenbrock, and James Vary for useful discussions. This work was supported by the U.S. Department of Energy, Office of Science, Office of Nuclear Physics, under Contracts No. DE-FG02-96ER40963 (University of Tennessee), No. DE-FG02-97ER41019 (University of North Carolina), No. DE-SC0008499 (NUCLEI SciDAC collaboration), NSERC Grant No. 401945-2011, and the Field Work Proposal ERKBP57 at Oak Ridge National Laboratory. Computer time was provided by the Innovative and Novel Computational Impact on Theory and Experiment (INCITE) program. TRIUMF receives funding via a contribution

through the National Research Council Canada. This research used resources of the Oak Ridge Leadership Computing Facility located in the Oak Ridge National Laboratory, which is supported by the Office of Science of the Department of Energy under Contract No. DE-AC05-00OR22725, and used computational resources of the National Center for Computational Sciences, the National Institute for Computational Sciences, and the Notur project in Norway.

*Note added.*—Very recently Bogner *et al.* [62] applied the in-medium similarity-renormalization-group method to construct nonperturbative shell-model interactions and applied it to neutron-rich oxygen isotopes.

- 
- [1] M. Stanoiu *et al.*, *Phys. Rev. C* **69**, 034312 (2004).  
 [2] R. Kanungo *et al.*, *Phys. Rev. Lett.* **102**, 152501 (2009).  
 [3] J. D. Holt, T. Otsuka, A. Schwenk, and T. Suzuki, *J. Phys. G* **39**, 085111 (2012).  
 [4] J. D. Holt, J. Menéndez, and A. Schwenk, *J. Phys. G* **40**, 075105 (2013).  
 [5] G. Hagen, M. Hjorth-Jensen, G. R. Jansen, R. Machleidt, and T. Papenbrock, *Phys. Rev. Lett.* **109**, 032502 (2012).  
 [6] D. Steppenbeck *et al.*, *J. Phys. Conf. Ser.* **445**, 012012 (2013).  
 [7] D. Steppenbeck *et al.*, *Nature (London)* **502**, 207 (2013).  
 [8] B. Wildenthal, *Prog. Part. Nucl. Phys.* **11**, 5 (1984).  
 [9] B. A. Brown and B. H. Wildenthal, *Annu. Rev. Nucl. Part. Sci.* **38**, 29 (1988).  
 [10] E. K. Warburton and B. A. Brown, *Phys. Rev. C* **46**, 923 (1992).  
 [11] M. Hjorth-Jensen, T. T. Kuo, and E. Osnes, *Phys. Rep.* **261**, 125 (1995).  
 [12] T. Otsuka, T. Suzuki, J. D. Holt, A. Schwenk, and Y. Akaishi, *Phys. Rev. Lett.* **105**, 032501 (2010).  
 [13] J. D. Holt, J. W. Holt, T. T. S. Kuo, G. E. Brown, and S. K. Bogner, *Phys. Rev. C* **72**, 041304 (2005).  
 [14] P. Navrátil, S. Quaglioni, I. Stetcu, and B. R. Barrett, *J. Phys. G* **36**, 083101 (2009).  
 [15] B. R. Barrett, P. Navrátil, and J. P. Vary, *Prog. Part. Nucl. Phys.* **69**, 131 (2013).  
 [16] P. Navrátil, M. Thoresen, and B. R. Barrett, *Phys. Rev. C* **55**, R573 (1997).  
 [17] A. F. Lisetskiy, B. R. Barrett, M. K. G. Kruse, P. Navrátil, I. Stetcu, and J. P. Vary, *Phys. Rev. C* **78**, 044302 (2008).  
 [18] D. Shukla, J. Engel, and P. Navrátil, *Phys. Rev. C* **84**, 044316 (2011).  
 [19] K. Tsukiyama, S. K. Bogner, and A. Schwenk, *Phys. Rev. C* **85**, 061304 (2012).  
 [20] F. Coester, *Nucl. Phys.* **7**, 421 (1958).  
 [21] F. Coester and H. Kümmel, *Nucl. Phys.* **17**, 477 (1960).  
 [22] J. Čížek, *J. Chem. Phys.* **45**, 4256 (1966).  
 [23] J. Čížek, *On the Use of the Cluster Expansion and the Technique of Diagrams in Calculations of Correlation Effects in Atoms and Molecules* (John Wiley & Sons, Inc., New York, 2007), pp. 35–89.  
 [24] H. Kümmel, K. H. Lührmann, and J. G. Zabolitzky, *Phys. Rep.* **36**, 1 (1978).  
 [25] G. Hagen, T. Papenbrock, M. Hjorth-Jensen, and D. J. Dean, arXiv:1312.7872.  
 [26] Y. Kondo *et al.*, *Phys. Rev. C* **79**, 014602 (2009).  
 [27] M. J. Strongman *et al.*, *Phys. Rev. C* **80**, 021302 (2009).  
 [28] A. Ozawa *et al.*, *Phys. Rev. C* **84**, 064315 (2011).  
 [29] N. Kobayashi *et al.*, *Phys. Rev. C* **86**, 054604 (2012).  
 [30] M. Petri *et al.*, *Phys. Rev. C* **86**, 044329 (2012).  
 [31] P. Voss *et al.*, *Phys. Rev. C* **86**, 011303 (2012).  
 [32] M. Petri *et al.*, *Phys. Rev. Lett.* **107**, 102501 (2011).  
 [33] C. Forssn, R. Roth, and P. Navrátil, *J. Phys. G* **40**, 055105 (2013).  
 [34] M. Stanoiu *et al.*, *Phys. Rev. C* **78**, 034315 (2008).  
 [35] K. Tanaka *et al.*, *Phys. Rev. Lett.* **104**, 062701 (2010).  
 [36] S. N. Ershov, J. S. Vaagen, and M. V. Zhukov, *Phys. Rev. C* **86**, 034331 (2012).  
 [37] D. R. Entem and R. Machleidt, *Phys. Rev. C* **68**, 041001 (2003).  
 [38] R. Machleidt and D. Entem, *Phys. Rep.* **503**, 1 (2011).  
 [39] P. Navrátil, *Few-Body Syst.* **41**, 117 (2007).  
 [40] D. Gazit, S. Quaglioni, and P. Navrátil, *Phys. Rev. Lett.* **103**, 102502 (2009).  
 [41] R. Roth, S. Binder, K. Vobig, A. Calci, J. Langhammer, and P. Navrátil, *Phys. Rev. Lett.* **109**, 052501 (2012).  
 [42] H. Hergert, S. Binder, A. Calci, J. Langhammer, and R. Roth, *Phys. Rev. Lett.* **110**, 242501 (2013).  
 [43] A. Cipollone, C. Barbieri, and P. Navrátil, *Phys. Rev. Lett.* **111**, 062501 (2013).  
 [44] E. D. Jurgenson, P. Navrátil, and R. J. Furnstahl, *Phys. Rev. Lett.* **103**, 082501 (2009).  
 [45] T. A. Lähde, E. Epelbaum, H. Krebs, D. Lee, U.-G. Meißner, and G. Rupak, *Phys. Lett. B* **732**, 110 (2014).  
 [46] G. Hagen, T. Papenbrock, D. J. Dean, A. Schwenk, A. Nogga, M. Włoch, and P. Piecuch, *Phys. Rev. C* **76**, 034302 (2007).  
 [47] P. Navrátil and B. R. Barrett, *Phys. Rev. C* **54**, 2986 (1996).  
 [48] S. A. Kucharski and R. J. Bartlett, *J. Chem. Phys.* **108**, 5243 (1998).  
 [49] A. G. Taube and R. J. Bartlett, *J. Chem. Phys.* **128**, 044110 (2008).  
 [50] J. R. Gour, P. Piecuch, M. Hjorth-Jensen, M. Włoch, and D. J. Dean, *Phys. Rev. C* **74**, 024310 (2006).  
 [51] G. R. Jansen, M. Hjorth-Jensen, G. Hagen, and T. Papenbrock, *Phys. Rev. C* **83**, 054306 (2011).  
 [52] G. R. Jansen, *Phys. Rev. C* **88**, 024305 (2013).  
 [53] R. J. Bartlett and M. Musiał, *Rev. Mod. Phys.* **79**, 291 (2007).  
 [54] S. Okubo, *Prog. Theor. Phys.* **12**, 603 (1954).  
 [55] K. Suzuki and S. Lee, *Prog. Theor. Phys.* **64**, 2091 (1980).  
 [56] K. Suzuki, *Prog. Theor. Phys.* **68**, 246 (1982).  
 [57] S. Kvaal, *Phys. Rev. C* **78**, 044330 (2008).  
 [58] F. Scholtz, H. Geyer, and F. Hahne, *Ann. Phys. (N.Y.)* **213**, 74 (1992).  
 [59] J. F. Stanton and R. J. Bartlett, *J. Chem. Phys.* **98**, 7029 (1993).  
 [60] G. Hagen, M. Hjorth-Jensen, G. R. Jansen, R. Machleidt, and T. Papenbrock, *Phys. Rev. Lett.* **108**, 242501 (2012).  
 [61] S. Baroni, P. Navrátil, and S. Quaglioni, *Phys. Rev. C* **87**, 034326 (2013).  
 [62] S. K. Bogner, H. Hergert, J. D. Holt, A. Schwenk, S. Binder, A. Calci, J. Langhammer, and R. Roth, preceding Letter, *Phys. Rev. Lett.* **113**, 142501 (2014).